HETEROCYCLES, Vol. 96, No. 6, 2018, pp. 1037 - 1052. © 2018 The Japan Institute of Heterocyclic Chemistry
Received, 12th February, 2018, Accepted, 27th April, 2018, Published online, 16th May, 2018
DOI: 10.3987/COM-18-13876

SYNTHESIS AND ANTIFUNGAL ACTIVITIES OF PYRIDINE BIOISOSTERES OF A BISMUTH HETEROCYCLE DERIVED FROM DIPHENYL SULFONE

A. F. M. Hafizur Rahman,[a] Toshihiro Murafuji,[a,b]* Kazuki Yamashita,[a] Masahiro Narita,[b] Isamu Miyakawa,[b] Yuji Mikata,[c] Katsuya Ishiguro,[b] and Shin Kamijo[b]

[a] Graduate School of Medicine, Yamaguchi University, Yamaguchi 753-8512, Japan. E-mail: murafuji@yamaguchi-u.ac.jp

[b] Graduate School of Sciences and Technology for Innovation, Yamaguchi University, Yamaguchi 753-8512, Japan.

[c] Department of Chemistry, Biology, and Environmental Science, Faculty of Science, Nara Women´s University, Nara 630-8506, Japan

Abstract – Heterocyclic iodobismuthanes **7**–**9** [IBi(C_6H_4-2-$SO_2C_5H_3$N-1´-)] derived from phenyl pyridinyl sulfones were synthesized. Their antifungal activities against the yeast *Saccharomyces cerevisiae* were compared with those of halobismuthanes [XBi(RC_6H_3-2-$SO_2C_6H_4$-1´-)] (**1**: X=Cl; **2**: X=I, R=H) derived from diphenyl sulfone derivatives to determine how the bioisosteric replacement of the benzene ring in **2** with the pyridine ring in **7**–**9** affects their activities. The antifungal activities of **7**–**9** were higher or comparable to those of **1** and **2**. The DFT calculations suggested that the generation of the antifungal activity of the bismuthanes was well understood by the nucleophilic addition of methanethiolate anion as a model biomolecule at the bismuth atom to give an intermediate ate complex.

INTRODUCTION

Bismuth is a heavy metal that is less toxic to human in comparison to the metals surrounding it in the periodic table.[1–3] This factor makes it possible to use bismuth compounds as drugs in the treatment of gastrointestinal disorders,[1] a red light-excitable photosensitizer in cells,[2] and biocompatible catalysts for ring opening polymerization.[3] Biologically active bismuth compounds have been the subject of considerable interest due to their medicinal utility.[4–13] We have reported the synthesis and antifungal

activity against the yeast *Saccharomyces cerevisiae* of bismuth heterocycles **1**–**3** (Scheme 1 and Table 2).[14–16]

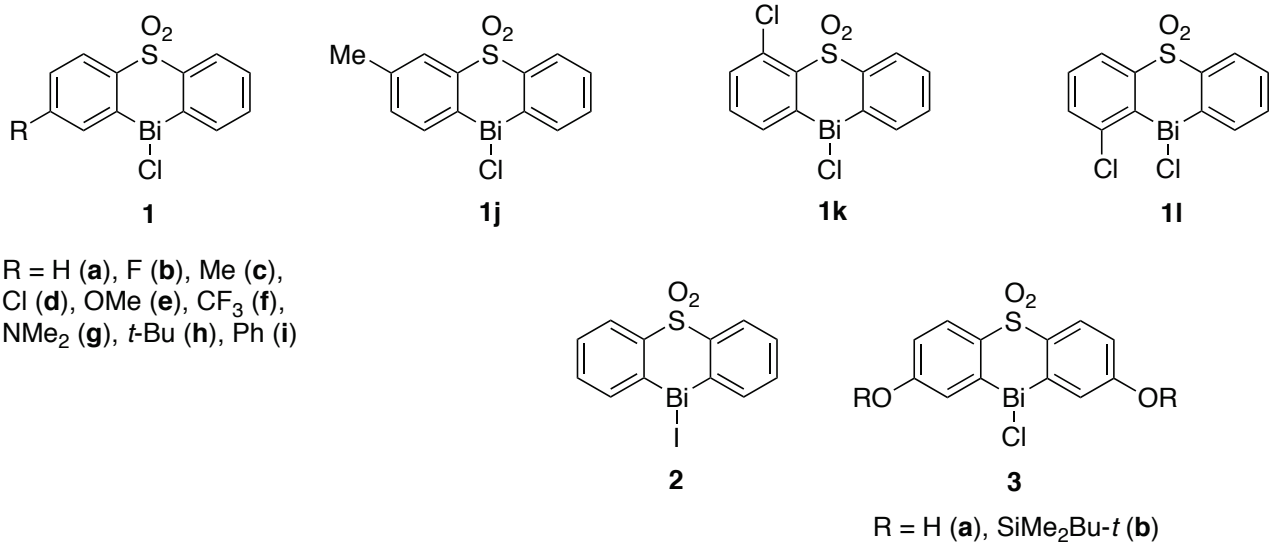

Scheme 1. Molecular structures of heterocyclic halobismuthanes **1**–**3**

The Lewis acidity at the bismuth center was essential for generating the activity. Halobismuthanes **1a**, **1b** and **2** showed high antifungal activities, and the activity of monosubstituted **1** decreased as the ClogP value increased, depending on the substituent. Based on this relationship, to achieve higher activity we synthesized **3a** bearing hydrophilic substituents, but its activity was much lower than that of parent **1a**.[15] We attributed this to the considerable decrease in the lipophilicity of **3a**. However, we have not tested this hypothesis experimentally.

We envisaged that replacing one of the benzene rings in **1a** or **2** with a pyridine ring should provide important information about whether the decrease in antifungal activity is related to the hydrophilicity. Pyridine is an isostere of benzene ring and is more hydrophilic than benzene.[17–22] We designed several bismuth heterocycles **4**–**9** derived from phenyl pyridinyl sulfone (Scheme 2).

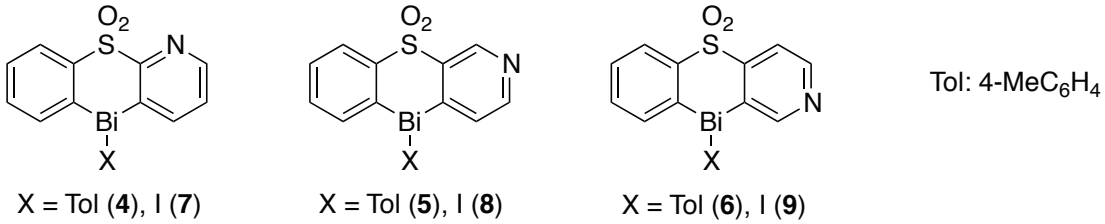

Scheme 2. Molecular structures of bismuth heterocycles **4**–**9**

This bioisosteric replacement is expected to make **7**–**9** much more hydrophilic than **2**, although the molecular shape is the same. In this paper, we report the synthesis and antifungal activities of **4**–**9**. To the best of our knowledge, organobismuth compounds in which the bismuth atom is directly attached to a

pyridine skeleton through a bismuth–carbon bond are rare and have been synthesized only recently.[23,24] In contrast, bismuth complexes with pyridine ligands bound through bismuth–nitrogen bonds have been characterized.[25–27]

RESULTS AND DISCUSSION

Synthesis: Phenyl 2-pyridinyl sulfone **10** was prepared by heating 2-bromopyridine and sodium benzenesulfinate in acetic acid.[28] Phenyl 3-pyridinyl sulfone **11**[29] and phenyl 4-pyridinyl sulfone **12**[30] were prepared by heating the corresponding bromopyridine and thiophenol in DMF in the presence of K_2CO_3 followed by the oxidation of the resulting phenyl pyridinyl sulfide.[31]

Our initial efforts were aimed at identifying conditions for the synthesis of **4** (Scheme 3). When **10** (1 mmol) was treated with LTMP (2.2 mmol) in THF at –40 °C for 20 min, an orange suspension was obtained. Addition of $TolBiCl_2$ (1 mmol) to the suspension at –70 °C, followed by workup and subsequent purification of the reaction mixture by chromatography (silica gel) gave **4** (0.68 mmol) in 68% yield along with acyclic **13** (0.048 mmol) in 10% yield as a minor product. The formation of **13** indicates that the pyridine-ring-lithiated intermediate of **10** is stable. Based on this result, we decided to lithiate **11** at a lower temperature because the lithiation of 3-substituted pyridines proceeds at the 4-position owing to the inherent higher acidity of the proton at this position.[32–34] Furthermore, the 4-position of the pyridine ring is susceptible to the unfavorable nucleophilic reaction.[35] When **11** was treated with LTMP at –55 °C, the solution immediately turned dark red. The reaction with $TolBiCl_2$ gave **5** in 40% yield. In this reaction, the bismuth analog, similar to **13** derived from the monolithiation of **11**, was not detected. Finally, we lithiated **12** under forcing conditions because the synthesis of **4** via the lithiation of **10** at –40 °C gave **13** derived from the monolithiation of **10**. Thus, **12** was lithiated with LTMP at –15 °C, and an orange suspension was obtained that was treated with $TolBiCl_2$ to give **6** in 58% yield without a byproduct, but unreacted **12** was recovered (35%). The recovery of **12** suggests that the pyridine ring proton adjacent to the sulfonyl group of **10** is susceptible to the lithiation compared to that of **12**. Iodination of **4**–**6** afforded the corresponding iodobismuthanes **7**–**9** in high yields together with 4-iodotoluene. This reaction may be rationalized as follows; the oxidative addition of iodine on the bismuth atom gives a pentavalent intermediate, which undergoes the reductive elimination of 4-iodotoluene to form the iodobismuthane. The selective elimination of the tolyl group is understood by the transannular interaction[36,37] between the bismuth and sulfonyl oxygen atoms, which forms the hypervalent O–Bi–I bond.[38] It is known that the transannular interaction promotes the reductive elimination on the pentavalent bismuth atom.[39,40] Furthermore, arsenic halogenation of 9-arsafluorene has shown that the reaction mechanism involves the oxidative addition and reductive elimination on the arsenic atom.[41]

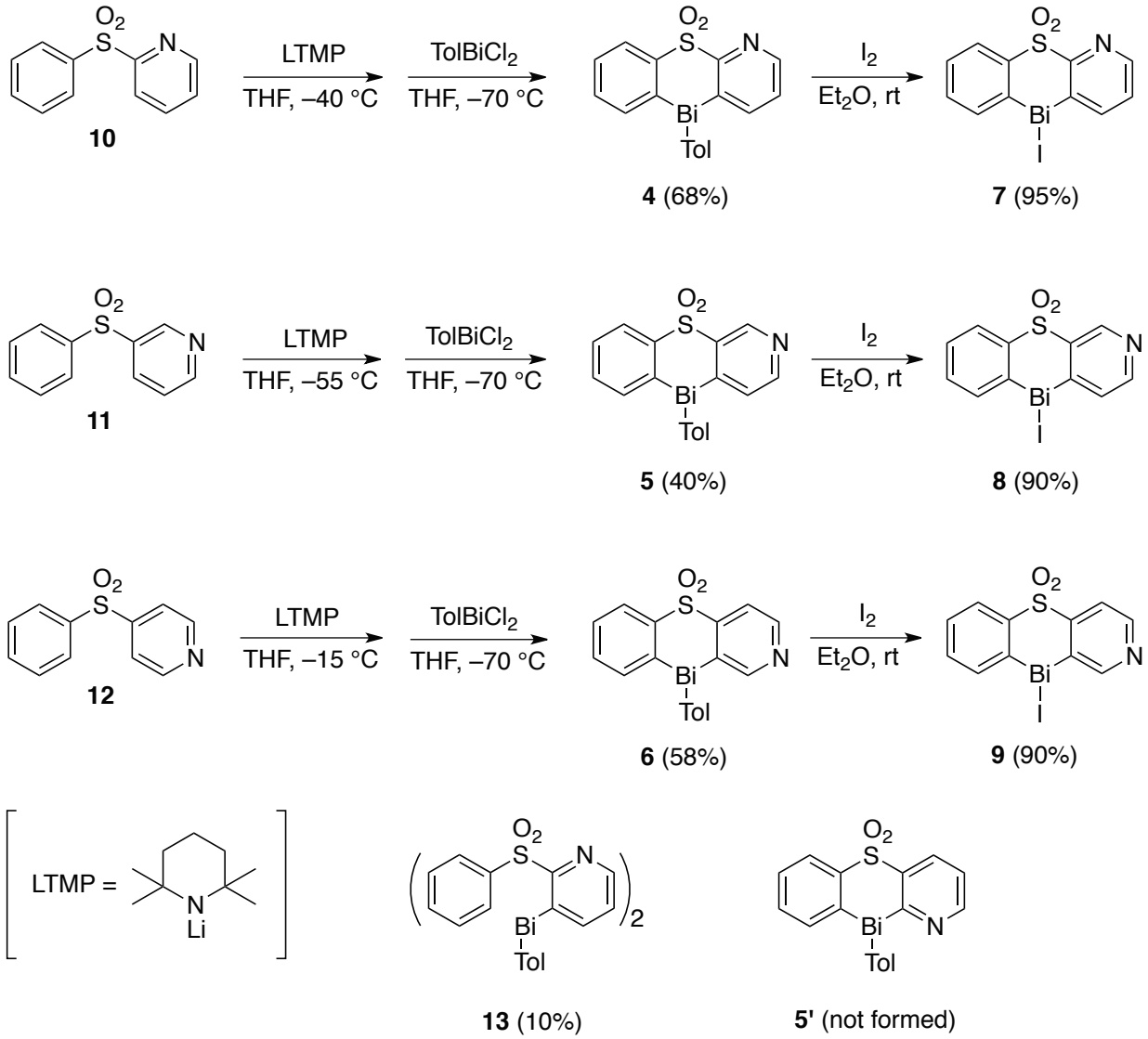

Scheme 3. Synthesis of bismuth heterocycles **4**–**9**

NMR spectroscopic study: The ^{1}H NMR spectra of compounds **4**–**6** in $CDCl_3$ showed characteristic proton signals due to the pyridine ring, which were used to assign these compounds. Compound **4** possesses only one proton adjacent to the nitrogen of the pyridine ring, whose signal appeared at the highest chemical shift (δ 8.63 ppm) as a double doublet. However, compound **5** showed signals from the two protons adjacent to the nitrogen, excluding the possibility of the formation of isomeric **5′**. In **5**, the signal of the unique pyridine ring proton next to the sulfonyl substituent appeared at a high chemical shift (δ 9.41 ppm) as a singlet owing to the effect of the adjacent nitrogen atom and the sulfonyl group. Compound **6** also shows the signals due to the two protons adjacent to the nitrogen. The signal for the pyridine ring proton neighboring the bismuth atom was characteristic of this compound and appeared as a singlet at a lower chemical shift (δ 8.84 ppm) than the singlet proton signal (δ 9.41 ppm) for the pyridine ring of **5**. In the ^{1}H NMR spectra of iodobismuthanes **7**–**9** in $CDCl_3$, the protons adjacent to the bismuth

atom in the benzene and pyridine rings underwent anisotropic deshielding because of their close proximity to the iodine atom.[9] Thus, the proton signal of the benzene ring for **7**–**9** appeared at about δ 9.2 ppm, 1.3 ppm higher than that of parent bismuthanes **4**–**6**. However, the proton signal of the pyridine ring for **7**, **8** and **9** appeared at higher shifts of δ 9.55, 9.13 and 9.89 ppm, respectively, which are 1.0–1.3 ppm higher than those of parent compounds **4**–**6**. These observations indicate that the sulfonyl oxygen atom was coordinated to the bismuth atom to form a hypervalent O–Bi–I bond. In the ^{13}C NMR spectra of iodobismuthanes **7**, **8** and **9** in DMSO-d_6, the signal for the ipso carbon attached to the bismuth in the pyridine ring appeared at δ 170.8, 188.4 and 169.7 ppm, respectively, whereas the signal due to the phenyl ipso carbon attached to the bismuth was always observed around δ 180 ppm.

X-Ray structure analysis of 9: We prepared single crystals of **9**. The molecular structure of **9** is shown in Figure 1, and the selected bond lengths, atomic distances and angles are shown in Table 1. This molecule has a chiral bismuth center. Interestingly, we found that only one enantiomer is present in the measured crystal.

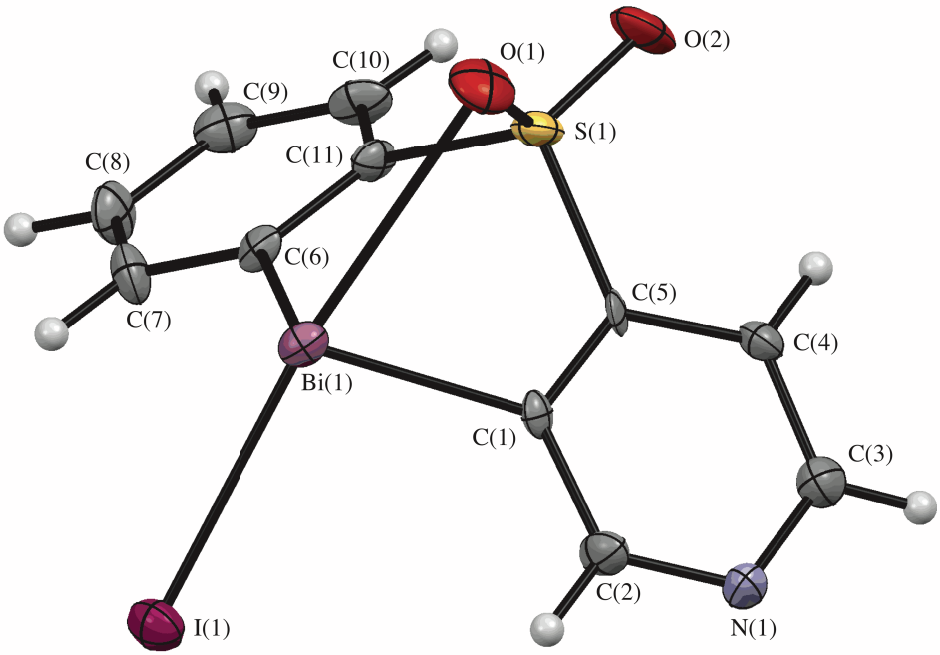

Figure 1. Molecular structure of **9**

The bismuth center adopts a distorted trigonal bipyramidal geometry, where the carbon atoms C(1) and C(6) occupy the equatorial plane with a C(1)–Bi(1)–C(6) angle of 86.1(5)° (Table 1). The apical positions of the distorted trigonal bipyramid are occupied by the sulfonyl oxygen and iodine atoms with an O(1)•••Bi(1)–I(1) angle of 159.0(2)°. The lone pair of electrons is considered to occupy the remaining equatorial position. The intramolecular Bi(1)•••O(1) distance 2.788(9) Å is longer than the sum of the

covalent radii (2.10 Å) but much shorter than that of the van der Waals radii (3.72 Å),[42,43] in accord with the formation of a hypervalent bond over the oxygen, bismuth and iodine atoms in **9**. The intermolecular atomic distances between the bismuth and nitrogen atoms and between the bismuth and iodine atoms are both within the sum of the van der Waals radii (3.62 and 4.05Å, respectively),[44] suggesting the existence of a weak interaction.

Table 1. Selected bond lengths (Å), atomic distances (Å) and angles (°) for compound **9**

Bond lengths		Torsion angles	
Bi(1)–I(1)	2.8518(12)	I(1)–Bi(1)–C(1)–C(2)	–43.3(9)
Bi(1)–C(1)	2.293(14)	Bi(1)–C(1)–C(2)–N(1)	–174.4(9)
Bi(1)–C(6)	2.294(14)	Bi(1)–C(1)–C(5)–S(1)	3.7(15)
S(1)–O(1)	1.485(16)	Bi(1)–C(1)–C(5)–C(4)	177.7(8)
S(1)–O(2)	1.435(11)	O(1)–S(1)–C(5)–C(1)	43.9(10)
		O(2)–S(1)–C(5)–C(1)	173.7(8)
		C(1)–Bi(1)–C(6)–C (7)	133.2(10)
Bond angles		Atomic distances	
C(1)–Bi(1)–C(6)	86.1(5)	intramolecular	
I(1)–Bi(1)–C(1)	96.1(3)	Bi(1)•••O(1)	2.788(9)
I(1)–Bi(1)–C(6)	92.8(3)		
O(1)•••Bi(1)–I(1)	159.0(2)	intermolecular	
Bi(1)–C(1)–C(5)	118.2(10)	Bi(1)•••N(1)	3.252(11)
C(5)–S(1)–C(11)	103.9(7)	Bi(1)•••I(1)	3.877(1)
O(1)–S(1)–O(2)	119.2(6)		

Qualitative antifungal assay: We tested the inhibition activity of iodobismuthanes **7**–**9** together with triarylbismuthanes **4**–**6** and **13**. Table 2 summarizes the inhibition activities of these compounds and our previously reported compounds **1**–**3**. Each compound was dissolved in DMSO at a concentration of 30 mM and 5 μL of each solution was directly spotted on the surface of the agar plate containing the yeast. Iodobismuthanes **7–9** were stable in water and DMSO, indicating that the hypervalent bond formation suppresses the hydrolysis and redistribution reactions of these compounds.

Triarylbismuthanes **4**–**6** and **13** were inactive, but iodobismuthanes **7**–**9** showed high antifungal activities. This is consistent with our previous finding that the Lewis acidic bismuth center is the active site.[9,14–16] The activity increased as the nitrogen atom moved further from the sulfonyl group and closer to the bismuth atom. Thus, iodobismuthane **9** showed the highest activity of **7**–**9** and higher activity than **1a** and **2**. The effect of the position of the nitrogen atom on the activity may imply an efficient secondary interaction of the nitrogen atom with biomolecules that bind to the active bismuth center. It has been reported that replacing the phenyl ring of the core indole with a pyridine ring preserves or substantially reduces the inhibitory activity, depending on the position of the nitrogen atom.[19]

Next, we investigated the effect of concentration of **9** on its antifungal activity. In response to decreasing

the concentrations of **9** from 30 to 3.75 mM, the activity decreased (20, 15, 13, and 10 mm for 30, 15, 7.5, and 3.75 mM, respectively). At the lowest concentration (3.75 mM), **9** still showed half of its original activity. Although the activities of **7**–**9** were not as high as the standard antifungal drug, nystatin, this finding demonstrates the high antifungal activity of organobismuth compounds.

Table 2. Antifungal assay for halobismuthanes and triarylbismuthanes

Compound	Inhibition Zone (mm)	ClogP	Compound	Inhibition Zone (mm)	ClogP
1a	18	1.18	**2**	17	1.18
1b	17	1.45	**3a**	8	0.81
1c	14	1.68	**3b**	0	6.13
1d	13	2.02	**4**	0	3.10
1e	11	1.52	**5**	0	3.10
1f	11	2.28	**6**	0	3.10
1g	7	1.77	**13**	0	6.29
1h	0	3.00	**7**	16	0.29
1i	0	3.06	**8**	19	0.29
1j	8	1.68	**9**	20	0.29
1k	10	2.02	Nystatin	30	–
1l	13	2.02			

We have previously reported the antifungal activity of chlorobismuthanes **1** and related derivatives **3**.[15] A clear structure–activity relationship was observed in **1a**–**l** (r = –0.85, n = 12) between the size of the inhibition zone and the value of ClogP, where the antifungal activity increased with decreasing lipophilicity (Table 2). However, **3a** (ClogP = 0.81), which was more hydrophilic, exhibited only low activity compared to **1a**. We attributed this to the considerable decrease in the lipophilicity of **3a** because the relationship appeared to be applied for the limited range of the ClogP values, depending on the substituent on the benzene ring. In fact, chlorobismuthanes **1h**, **1i** and **3b**, whose value of ClogP was more lipophilic and over 3.00, did not show any antifungal activities despite the presence of the Lewis acidic bismuth center. Hence, taking into account the fact that the activity of **3a** was lower than that of **1a**, it was unexpected that more hydrophilic **7**–**9** (ClogP = 0.29) showed higher activities than **3a**. Furthermore, Figure 2 revealed that application of the data on **2** and **7**–**9** to the plot of **1** improved the linearity of the correlation (r = –0.86, n = 16). Although the reason for the considerable deviation of **3a** from this plot is not clear, it may be attributed to the acidic phenolic hydroxy substituents which ionize or aggregate through the intermolecular hydrogen bonding, preventing **3a** from passing through the cell membrane of the yeast.

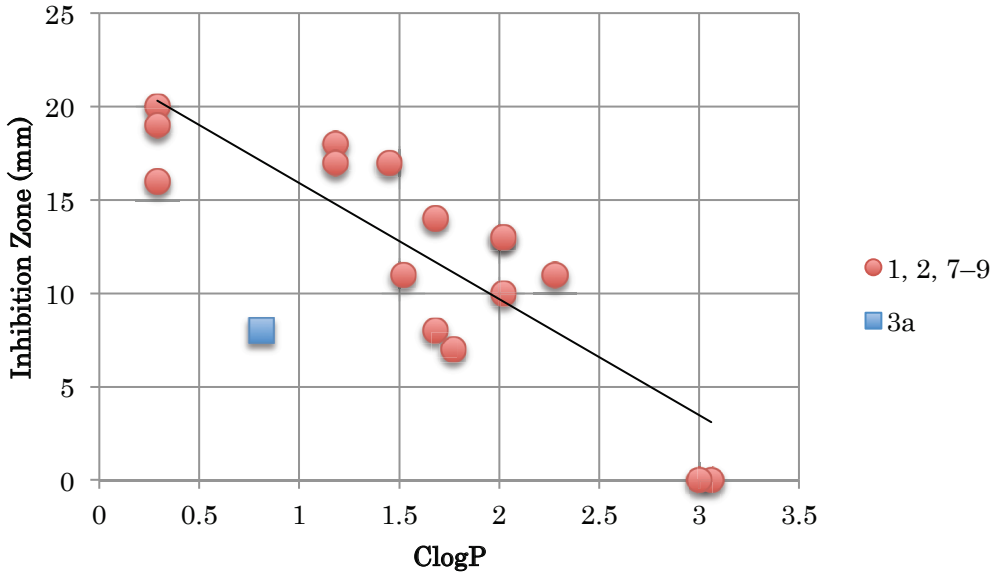

Figure 2. Structure–activity relationship for halobismuthanes **1**, **2**, **3a** and **7–9**

DFT study: Recently, we have reported the antifungal activity of hypervalent organobismuth(III) compounds derived from alkyl aryl ketones against *S. cerevisiae*.[9] Bismuthane **14** showed the highest activity comparable to **1a**, but **15** bearing a bulky mesityl group was inactive (Scheme 4). Furthermore, DFT calculations[45] suggested that the generation of antifungal activity of the bismuthanes was well understood by the nucleophilic addition of a biomolecule at the bismuth atom to give an intermediate ate complex (Table 3).[9] Although we have not identified the biomolecules to which these bismuthanes bind, we expect that the Lewis acidic bismuth atom has a high affinity for thiol groups.[1,46] There was a weak but positive correlation between the antifungal activity and the association energy (enthalpy) in the ate complex formation using methanethiolate anion as a model nucleophile.[9] Thus, the reactions of **1a**, **2** and **14** had high exothermic association energies while no minimum energy path connects the reactants and the product in the reaction of **15** bearing a bulky mesityl group.

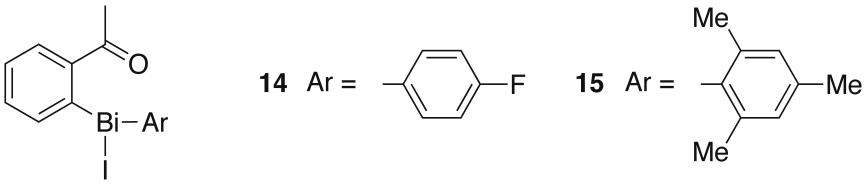

Scheme 4. Structures of iodobismuthanes **14** and **15**

It should be noted that the association energy of **3a** was almost the same as that of **1a**. This indicates that the hydroxy substituents little affect the ate complex formation of **3a**. Despite this, the loss of the activity in **3a** may be attributed to the behavior of the phenolic hydroxy substituents mentioned above.

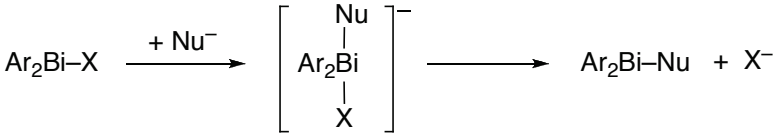

Table 3. Association energy of halobismuthanes

Compound	Inhibition Zone (mm)	Association Energy (kcal/mol)
1a	18	–17.22
2	17	–20.18
3a	8	–17.15
14	19	–16.00
15	0	–
7	16	–20.87
8	19	–21.54
9	20	–21.95

We calculated the association energy of **7–9** by using methanethiolate anion as a model nucleophile (Table 3 and Scheme 5). It is expected that the intramolecular bismuth–oxygen coordination is cleaved by the ate complex formation to form a hypervalent S–Bi–I bond. Iodobismuthanes **7–9** had some of the most exothermic association reactions. Interestingly, the association energy negatively increased in the order **7** < **8** < **9**, which is in good agreement with the order of the antifungal activity. Hence, this association path is preferable to understand the mechanism of action of these iodobismuthanes.

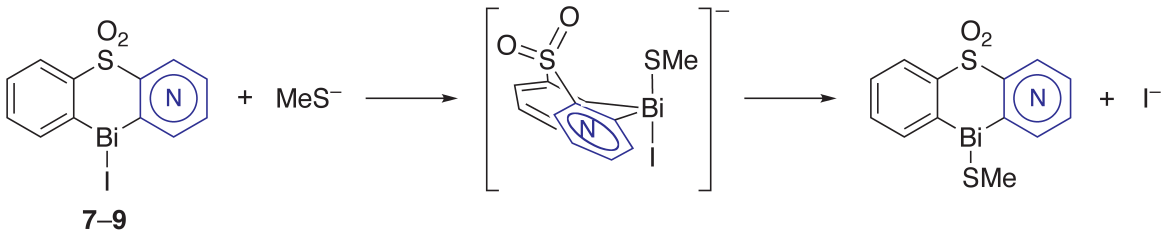

Scheme 5. Plausible association pathway of iodobismuthanes **7–9** using methanethiolate anion

CONCLUSION

The bioisosteric replacement of the phenyl ring of the diphenyl sulfone scaffold by the pyridine ring improved the antifungal activity of the hypervalent halobismuthanes. A clear structure–activity relationship was observed in **1**, **2** and **7–9** between the size of the inhibition zone and the value of ClogP. Stabilizing the ate complex appears to be important. The present study provides insights that will aid the design of antifungal hypervalent halobismuthanes by simply estimating the ClogP value and the association energy. Further studies are now underway to find more active halobismuthanes.

EXPERIMENTAL

All reactions were carried out under argon unless otherwise noted. THF and Et_2O were distilled from benzophenone ketyl before use. Melting points were determined on a YANAGIMOTO melting point apparatus without correction. ^1H and ^{13}C NMR spectra were recorded in $CDCl_3$ or DMSO-d_6 on a BRUKER AVANCE 400S spectrometer. Chemical shifts were referenced to residual solvent peak: $CHCl_3$ (7.26 ppm, 77.0 ppm) and DMSO (2.50 ppm, 40.45 ppm). IR spectra were obtained as KBr pellets on a Nicolet FT-IR Impact 410 spectrophotometer. Elemental analyses were performed on a MICRO CORDER JM10 apparatus (J-SCIENCE LAB. Co.). HRMS were recorded on a Bruker Daltonics micrOTOF II (APCI) instrument. Charts of ^1H and ^{13}C NMR spectra of reported compounds are summarized in Supporting Information.

Synthesis of 4 and 13: A mixture of bismuth(III) chloride (211 mg, 0.67 mmol) and tris(4-methylphenyl)bismuthane (162 mg, 0.33 mmol) was stirred in Et_2O (8 mL) at room temperature for 1 h. To a stirred solution of 2,2,6,6-tetramethylpiperidine (0.37 mL, 2.2 mmol) in THF (10 mL) was added dropwise at –78 °C butyllithium (2.2 mmol). After 50 min a solution of **10** (219 mg, 1 mmol) in THF (3 mL) was added at –40 °C and the mixture was stirred for 20 min at this temperature. To this solution was added at –70 °C the suspension of dichloro(4-methylphenyl)bismuthane (ca. 1 mmol) thus formed, and the resulting mixture was stirred for 2 h, during which time the temperature was raised to ambient. The reaction mixture was poured into brine (50 mL) and extracted with EtOAc (50 mL × 3). The combined extracts were concentrated to leave an oily residue, which was purified by chromatography (silica gel) using hexane–EtOAc (3:1) as the eluent to afford **4** and **13** in 68% yield (352 mg, 0.68 mmol) and 10% yield (35 mg, 0.048 mmol), respectively.

4-Aza-10-(4-methylphenyl)phenothiabismine 5,5-dioxide (4): colorless solid; mp 232–234 °C; ^1H NMR (400 MHz, $CDCl_3$): δ 2.35 (3H, s), 7.19 (1H, dd, J = 4.8, 7.4 Hz), 7.26 (2H, d, J = 7.6 Hz), 7.41 (1H, dt, J = 1.2, 7.2 Hz), 7.45 (1H, dt, J = 1.2, 7.2 Hz), 7.63 (2H, d, J = 7.6 Hz), 7.87 (1H, dd, J = 1.2, 7.6 Hz), 8.21 (1H, dd, J = 1.6, 7.2 Hz), 8.43 (1H, dd, J = 1.2, 7.6 Hz), 8.63 (1H, dd, J = 1.6, 4.4 Hz); ^{13}C NMR (100 MHz, $CDCl_3$): δ 21.6, 127.3, 128.3, 129.0, 132.0, 133.8, 137.5, 138.6, 138.9, 141.9, 146.1, 149.0, 151.3 (br), 157.6, 159.2 (br), 163.1 (br). IR (KBr): ν = 1310, 1290, 1160, 1130, 1100, 1080, 1050, 1010, 790, 760, 590 and 570 cm^{-1}. Anal. Calcd for $C_{18}H_{14}BiNO_2S$: C, 41.79; H, 2.73; N, 2.71. Found: C, 41.97; H, 3.03; N, 2.66.

(4-Methylphenyl)bis(2-phenylsulfonylpyridin-3-yl)bismuthane (13): colorless solid; mp 229–231 °C; ^1H NMR (400 MHz, $CDCl_3$): δ 2.36 (3H, s), 7.26 (2H, d, J = 7.6 Hz), 7.28 (2H, dd, J = 4.8, 7.4 Hz), 7.43 (4H, t, J = 7.6 Hz), 7.56 (2H, t, J = 7.2 Hz), 7.60 (2H, d, J = 7.6 Hz), 7.86 (4H, d, J = 7.2 Hz), 8.20 (2H, dd, J = 1.6, 7.6 Hz), 8.74 (2H, dd, J = 1.6, 4.4 Hz); ^{13}C NMR (100 MHz, $CDCl_3$): δ 21.6, 128.9, 129.0 (×2), 132.3, 133.6, 138.0, 138.1, 139.2, 149.3, 149.7, 157.2 (br), 162.6, 168.5 (br). IR (KBr): ν = 1450,

1300, 1160, 1120, 1080, 770, 750, 740, 710, 690, 590 and 570 cm^{-1}. Anal. Calcd for $C_{29}H_{23}BiN_2O_4S_2$: C, 47.29; H, 3.15; N, 3.80. Found: C, 46.90; H, 3.47; N, 3.79.

3-Aza-10-(4-methylphenyl)phenothiabismine 5,5-dioxide (5): A mixture of bismuth(III) chloride (211 mg, 0.67 mmol) and tris(4-methylphenyl)bismuthane (162 mg, 0.33 mmol) was stirred in Et_2O (8 mL) at room temperature for 1 h. To a stirred solution of 2,2,6,6-tetramethylpiperidine (0.37 mL, 2.2 mmol) in THF (10 mL) was added dropwise at –78 °C butyllithium (2.2 mmol). After 20 min a solution of **11** (219 mg, 1 mmol) in THF (3 mL) was added at –55 °C, and the temperature was lowered to –70 °C immediately. To this solution was added at this temperature the suspension of dichloro(4-methylphenyl)bismuthane (ca. 1 mmol) thus formed, and the resulting mixture was stirred for 2 h, during which time the temperature was raised to ambient. The reaction mixture was poured into brine (50 mL) and extracted with EtOAc (50 mL × 3). The combined extracts were concentrated to leave an oily residue, which was purified by chromatography (silica gel) using hexane–EtOAc (3:1) as the eluent to afford **5** in 40% yield (207 mg, 0.4 mmol). Colorless solid; mp 224–226 °C; ^{1}H NMR (400 MHz, $CDCl_3$): δ 2.35 (3H, s), 7.27 (2H, d, J = 7.2 Hz), 7.39 (1H, dt, J = 1.2, 7.2 Hz), 7.44 (1H, dt, J = 1.2, 7.2 Hz), 7.63 (2H, d, J = 7.2 Hz), 7.80 (1H, d, J = 4.4 Hz), 7.89 (1H, dd, J = 1.2, 7.2 Hz), 8.42 (1H, dd, J = 1.6, 7.6 Hz), 8.44 (1H, d, J = 4.4 Hz), 9.41 (1H, s); ^{13}C NMR (100 MHz, $CDCl_3$): δ 21.6, 127.4, 128.6, 132.1, 132.3, 133.9, 137.7, 138.6, 138.7, 139.1, 141.2, 146.3, 152.5, 158.9 (br), 162.4 (br), 168.7 (br). IR (KBr): ν = 1550, 1440, 1390, 1300, 1150, 1100, 1080, 1060, 1010, 780, 760, 730, 600, 570, 520 and 460 cm^{-1}. Anal. Calcd for $C_{18}H_{14}BiNO_2S$: C, 41.79; H, 2.73; N, 2.71. Found: C, 41.93; H, 3.09; N, 2.70.

2-Aza-10-(4-methylphenyl)phenothiabismine 5,5-dioxide (6): A mixture of bismuth(III) chloride (211 mg, 0.67 mmol) and tris(4-methylphenyl)bismuthane (162 mg, 0.33 mmol) was stirred in Et_2O (8 mL) at room temperature for 1 h. To a stirred solution of 2,2,6,6-tetramethylpiperidine (0.37 mL, 2.2 mmol) in THF (10 mL) was added dropwise at –78 °C butyllithium (2.2 mmol). After 50 min a solution of **12** (219 mg, 1 mmol) in THF (3 mL) was added at –15 °C, and the mixture was stirred for 10 min at this temperature. To this solution was added at –70 °C the suspension of dichloro(4-methylphenyl)bismuthane (ca. 1 mmol) thus formed, and the resulting mixture was stirred for 2 h, during which time the temperature was raised to ambient. The reaction mixture was poured into brine (50 mL) and extracted with EtOAc (50 mL × 3). The combined extracts were concentrated to leave an oily residue, which was purified by chromatography (silica gel) using hexane–EtOAc (3:1) as the eluent to afford **6** in 58% yield (301 mg, 0.58 mmol). Colorless solid; mp 100–102 °C; ^{1}H NMR (400 MHz, $CDCl_3$): δ 2.34 (3H, s), 7.26 (2H, d, J = 7.6 Hz), 7.39 (1H, dt, J = 1.2, 7.2 Hz), 7.44 (1H, dt, J = 1.2, 7.2 Hz), 7.65 (2H, d, J = 7.6 Hz), 7.90 (1H, dd, J = 0.8, 7.6 Hz), 8.17 (1H, d, J = 5.2 Hz), 8.41 (1H, dd, J = 0.8, 7.6 Hz), 8.69 (1H, d, J = 4.4 Hz), 8.84 (1H, s); ^{13}C NMR (100 MHz, $CDCl_3$): δ 21.6, 120.3, 127.8, 128.5, 132.0, 134.0, 137.9, 138.5, 139.0, 140.3, 150.2 (×2), 150.6 (br), 157.4, 158.8 (br), 160.8 (br). IR (KBr): ν = 1540, 1490, 1450, 1390,

1300, 1170, 1150, 1100, 1060, 1010, 790, 750, 730, 690, 590, 570 and 480 cm^{-1}. Anal. Calcd for $C_{18}H_{14}BiNO_2S$: C, 41.79; H, 2.73; N, 2.71. Found: C, 41.81; H, 3.03; N, 2.67.

Synthesis of 7, 8 and 9: A typical example is exemplified by the synthesis of **7**: To a suspension of **4** (104 mg, 0.2 mmol) in Et_2O (5 mL) was added dropwise a solution of iodine (51 mg, 0.2 mmol) in the same solvent (5 mL) at room temperature until **4** was completely consumed (checked by TLC). The reaction mixture was concentrated to leave solids, which were crystallized from MeOH to give **7**.

4-Aza-10-iodophenothiabismine 5,5-dioxide (7): pale yellow solid; yield 95%; mp > 307 °C; ^{1}H NMR (400 MHz, $CDCl_3$): δ 7.45 (1H, dd, J = 4.8, 7.6 Hz), 7.54 (1H, t, J = 7.6 Hz), 7.69 (1H, t, J = 7.6 Hz), 8.36 (1H, d, J = 7.2 Hz), 8.74 (1H, d, J = 4.8 Hz), 9.21 (1H, d, J = 7.2 Hz), 9.55 (1H, d, J = 7.6 Hz); ^{13}C NMR (100 MHz, DMSO-d_6): δ 128.9, 129.1, 130.3, 136.9, 141.9 (×2), 149.4, 150.3, 158.3, 170.8, 179.6. IR (KBr): ν = 1550, 1300, 1150, 1130, 1100, 1070, 1010, 750, 740, 640, 590, 570, 510 and 460 cm^{-1}. HRMS (APCI): *m/z* $[M+H]^+$ calcd for $C_{11}H_8BiINO_2S$: 553.9119; found: 553.9110.

3-Aza-10-iodophenothiabismine 5,5-dioxide (8): pale yellow solid; yield 90%; mp 305–307 °C (decomp.); ^{1}H NMR (400 MHz, $CDCl_3$): δ 7.55 (1H, t, J = 7.6 Hz), 7.67 (1H, t, J = 7.2 Hz), 8.38 (1H, d, J = 7.6 Hz), 8.82 (1H, d, J = 4.4 Hz), 9.13 (1H, d, J = 4.8 Hz), 9.22 (1H, d, J = 7.2 Hz), 9.44 (1H, s); ^{13}C NMR (100 MHz, DMSO-d_6): δ 127.6, 129.4, 136.2, 137.0, 139.2, 141.7, 142.1, 145.7, 155.3, 180.2 (br), 188.4 (br). IR (KBr): ν = 1560, 1290, 1150, 1130, 1100, 1080 and 1020 cm^{-1}. HRMS (APCI): *m/z* $[M+H]^+$ calcd for $C_{11}H_8BiINO_2S$: 553.9119; found: 553.9123.

2-Aza-10-iodophenothiabismine 5,5-dioxide (9): pale yellow solid; yield 90%; mp 232–234 °C (decomp.); ^{1}H NMR (400 MHz, $CDCl_3$): δ 7.53 (1H, t, J = 7.2 Hz), 7.67 (1H, t, J = 7.2 Hz), 8.08 (1H, d, J = 4.8 Hz), 8.35 (1H, d, J = 7.6 Hz), 8.84 (1H, d, J = 4.8 Hz), 9.25 (1H, d, J = 7.2 Hz), 9.89 (1H, s); ^{13}C NMR (100 MHz, DMSO-d_6): δ 120.3, 128.0, 129.4, 137.1, 140.8, 142.3, 150.6, 150.7, 161.8, 169.7, 179.6. IR (KBr): ν = 1550, 1390, 1320, 1290, 1270, 1170, 1150, 1120, 1090, 840, 750, 590, 570, 520 and 470 cm^{-1}. Anal. Calcd for $C_{11}H_7BiINO_2S$: C, 23.89; H, 1.28; N, 2.53. Found: C, 23.89; H, 1.50; N, 2.47.

Qualitative antifungal assay: The yeast *S. cerevisiae* W303-1A (*MAT***a** *ade2-1 can1-100 ura3-1 leu2-3,112 trp1-1 his3-11,15*) was used for the qualitative antifungal assay. Yeast extract-peptone-dextrose (YPD) plates contained 1% yeast extract, 2% peptone, 2% glucose and 1.2% agar. The cells were inoculated at a concentration of 1.3×10^4 cells/mL in YPD agar medium at 48 °C and YPD plates were immediately made in Petri dishes. Each compound was dissolved in dimethyl sulfoxide (DMSO) at a concentration of 30 mM and 5 μL of each solution was directly spotted on the surface of the plate. The plates were incubated for 24 h at 30 °C and antifungal activity was indicated by the presence of clear inhibition zones around the spot. The control experiment showed that DMSO does not inhibit fungal

growth at all. In order to know the error on the inhibition zone, we carried out the antifungal assay of compounds many times and confirmed that the error was within ±1 mm.

Lipophilicity: The calculated logarithms of water-octanol partition coefficients (ClogP values) were obtained from the ClogP tool in ChemDraw Ultra 11.0 (CambridgeSoft, Cambridge, MA, USA).

DFT calculation of the association energies: The geometries of the bismuth compounds and the corresponding MeS^--adduct anions in Table 3 were fully optimized in water through density functional theory (DFT) calculations within the polarizable continuum model (PCM) using the Gaussian 09 program package.[45] The hybrid B3LYP exchange-correlation functional and 6-31+G*/lanl2dz mixed basis set (lanl2dz effective core potential for bismuth and iodine and 6-31+G* basis set for the remaining atoms) were employed. All d functions in 6-31+G* are pure 5 D basis functions, which is the default form in the Gaussian 09 GenECP calculations. The exothermicity for the nucleophilic addition of MeS^- was calculated from the energies in water of each substrate, in which only the most stable conformer with the lowest energy was considered.

X-Ray crystallographic study: A colorless crystal of **9** was mounted on a glass fiber. All measurements were made with a Rigaku Mercury 70 diffractometer using graphite monochromated Mo-Kα radiation. The data were collected at a temperature of –119 ± 1 °C to a maximum 2θ value of 55.0°. The structure was solved by direct methods[47] and expanded using Fourier techniques. The non-hydrogen atoms were refined anisotropically. All calculations were performed using the CrystalStructure[48] crystallographic software package except for refinement, which was performed using SHELXL Version 2016/6.[49] Crystal data, data collection summary and refinement parameters of **9** are given in Supporting Information. Deposition number CCDC-1836491 for compound **9**. Free copies of the data can be obtained via http://www.ccdc.cam.ac.uk/conts/retrieving.html (or from the Cambridge Crystallographic Data Centre, 12 Union Road, Cambridge, CB2 1EZ, UK; Fax: +44 1223 336033; e-mail: deposit@ccdc.cam.ac.uk).

ACKNOWLEDGEMENTS

We are grateful to the Center of Instrumental Analysis, Yamaguchi University and the Tokiwa Instrumentation Analysis Center, Yamaguchi University.

REFERENCES

1. Y. Hong, Y.-T. Lai, G. C.-F. Chan, and H. Sun, *Proc. Natl. Acad. Sci. USA*, 2015, **112**, 3211.
2. T. Hirayama, A. Mukaimine, K. Nishigaki, H. Tsuboi, S. Hirosawa, K. Okuda, M. Ebihara, and H. Nagasawa, *Dalton Trans*., 2017, **46**, 15991.
3. C. Bonné, A. Pahwa, C. Picard, and M. Visseaux, *Inorg. Chim. Acta*, 2017, **455**, 521.
4. D. M. Keogan and D. M. Griffith, *Molecules*, 2014, **19**, 15258.

5. H. Li and H. Sun, *Curr. Opin. Chem. Biol.*, 2012, **16**, 74.
6. G. G. Briand and N. Burford, *Chem. Rev.*, 1999, **99**, 2601.
7. Y. C. Ong, V. L. Blair, L. Kedzierski, K. L. Tuck, and P. C. Andrews, *Dalton Trans.*, 2015, **44**, 18215.
8. A. Islam, B. L. Rodrigues, I. M. Marzano, E. C. Perreira-Maia, D. Dittz, M. T. Paz Lopes, M. Ishfaq, F. Frézard, and C. Demicheli, *Eur. J. Med. Chem.*, 2016, **109**, 254.
9. T. Murafuji, M. Tomura, K. Ishiguro, and I. Miyakawa, *Molecules*, 2014, **19**, 11077.
10. K. Onishi, M. Douke, T. Nakamura, Y. Ochiai, N. Kakusawa, S. Yasuike, J. Kurita, C. Yamamoto, M. Kawahata, K. Yamaguchi, and T. Yagura, *J. Inorg. Biochem.*, 2012, **117**, 77.
11. I. P. Ferreira, E. D. L. Piló, A. A. Recio-Despaigne, J. G. Da Silva, J. P. Ramos, L. B. Marques, P. H. D. M. Prazeres, J. A. Takahashi, E. M. Souza-Fagundes, W. Rocha, and H. Beraldo, *Bioorg. Med. Chem.*, 2016, **24**, 2988.
12. D. H. A. Ishak, K. K. Ooi, K.-P. Ang, A. M. Akim, Y.-K. Cheah, N. Nordin, S. N. B. A. Halim, H.-L. Seng, and E. R. T. Tiekink, *J. Inorg. Biochem.*, 2014, **130**, 38.
13. M. Li, Y. Lu, M. Yang, Y. Li, L. Zhang, and S. Xie, *Dalton Trans*., 2012, **41**, 12882.
14. T. Murafuji, Y. Miyoshi, M. Ishibashi, A. F. M. Mustafizur Rahman, Y. Sugihara, I. Miyakawa, and H. Uno, *J. Inorg. Biochem.*, 2004, **98**, 547.
15. T. Murafuji, Y. Fujiwara, D. Yoshimatsu, I. Miyakawa, K. Migita, and Y. Mikata, *Eur. J. Med. Chem.*, 2011, **46**, 519.
16. T. Murafuji, K. Kitagawa, D. Yoshimatsu, K. Kondo, K. Ishiguro, R. Tsunashima, I. Miyakawa, and Y. Mikata, *Eur. J. Med. Chem.*, 2013, **63**, 531.
17. B. Kelly, M. McMullan, C. Muguruza, J. E. Ortega, J. Javier Meana, L. F. Callado, and I. Rozas, *J. Med. Chem.*, 2015, **58**, 963.
18. K. Miyata, G. Möller, D. Schepmann, and B. Wünsch, *Bioorg. Med. Chem.*, 2014, **22**, 4277.
19. T. Wang, Z. Yin, Z. Zhang, J. A. Bender, Z. Yang, G. Johnson, Z. Yang, L. M. Zadjura, C. J. D'Arienzo, D. DiGiugno Parker, C. Gesenberg, G. A. Yamanaka, Y.-F. Gong, H.-T. Ho, H. Fang, N. Zhou, B. V. McAuliffe, B. J. Eggers, L. Fan, B. Nowicka-Sans, I. B. Dicker, Q. Gao, R. J. Colonno, P.-F. Lin, N. A. Meanwell, and J. F. Kadow, *J. Med. Chem.*, 2009, **52**, 7778.
20. R. H. Bahekar, M. R. Jain, P. A. Jadav, A. Goel, D. N. Patel, V. M. Prajapati, A. A. Gupta, H. Modi, and P. R. Patel, *Bioorg. Med. Chem.*, 2007, **15**, 5950.
21. D. Laeckmann, F. Rogister, J.-V. Dejardin, C. Prosperi-Meys, J. Géczy, J. Delarge, and B. Masereel, *Bioorg. Med. Chem.*, 2002, **10**, 1793.
22. K. Yoshino, T. Kohno, T. Morita, and G. Tsukamoto, *J. Med. Chem.*, 1989, **32**, 1528.

23. K. Urgin, C. Aubé, C. Pichon, M. Pipelier, V. Blot, C. Thobie-Gautier, E. Léonel, D. Dubreuil, and S. Condon, *Tetrahedron Lett.*, 2012, **53**, 1894.
24. M. Hébert, P. Petiot, E. Benoit, J. Dansereau, T. Ahmad, A. Le Roch, X. Ottenwaelder, and A. Gagnon, *J. Org. Chem*., 2016, **81**, 5401.
25. S. C. James, N. C. Norman, A. G. Orpen, and J. Starbuck, *CrystEngComm.*, 2000, **2**, 67.
26. S. C. James, N. C. Norman, and A. G. Orpen, *J. Chem. Soc., Dalton Trans.*, 1999, 2837.
27. M. Ali, W. R. McWhinnie, A. A. West, and T. A. Hamor, *J. Chem. Soc., Dalton Trans.*, 1990, 899.
28. B. Qu, L. P. Samankumara, J. Savoie, D. R. Fandrick, N. Haddad, X. Wei, S. Ma, H. Lee, S. Rodriguez, C. A. Busacca, N. K. Yee, J. J. Song, and C. H. Senanayake, *J. Org. Chem.*, 2014, **79**, 993.
29. N. Margraf and G. Manolikakes, *J. Org. Chem.*, 2015, **80**, 2582.
30. J. Zou, F. Li, and F. G. Tao, *Chin. Chem. Lett.*, 2009, **20**, 17.
31. W. G. Trankle and M. E. Kopach, *Org. Process Res. Dev.*, 2007, **11**, 913.
32. G. Rouquet, D. C. Blakemore, and S. V. Ley, *Chem. Commun.*, 2014, **50**, 8908.
33. G. Deguest, A. Devineau, L. Bischoff, C. Fruit, and F. Marsais, *Org. Lett.*, 2006, **8**, 5889.
34. N. Furukawa, T. Shibutani, and H. Fujihara, *Tetrahedron Lett.*, 1989, **30**, 7091.
35. A. I. Meyers and R. A. Gabel, *Heterocycles*, 1978, **11**, 133.
36. K. Ohkata, M. Ohnishi, and K.-y. Akiba, *Tetrahedron Lett.*, 1988, **29**, 5401.
37. K. Ohkata, S. Takemoto, M. Ohnishi, and K.-y. Akiba, *Tetrahedron Lett.*, 1989, **30**, 4841.
38. H. Suzuki, T. Murafuji, and N. Azuma, *J. Chem. Soc., Perkin Trans. 1*, 1992, 1593.
39. M. Minoura, Y. Kanamori, A. Miyake, and K.-y. Akiba, *Chem. Lett.*, 1999, **28**, 861.
40. N. Sakurai and T. Mukaiyama, *Chem. Lett.*, 2007, **36**, 928.
41. S. Tanaka, H. Imoto, T. Yumura, and K. Naka, *Organometallics*, 2017, **36**, 1684.
42. T. Murafuji, T. Mutoh, K. Satoh, K. Tsunenari, N. Azuma, and H. Suzuki, *Organometallics*, 1995, **14**, 3848.
43. A. Bondi, *J. Phys. Chem.*, 1964, **68**, 441.
44. M. Mantina, A. C. Chamberlin, R. Valero, C. J. Cramer, and D. G. Truhlar, *J. Phys. Chem. A*, 2009, **113**, 5806.
45. M. J. Frisch, G. W. Trucks, H. B. Schlegel, G. E. Scuseria, M. A. Robb, J. R. Cheeseman, G. Scalmani, V. Barone, B. Mennucci, and G. A. Petersson, *et al.* Gaussian 09, Revision C.01; Gaussian, Inc.: Wallingford, CT, USA, 2010.
46. N. Burford, M. D. Eelman, D. E. Mahony, and M. Morash, *Chem. Commun.*, 2003, 146.
47. SIR92: A. Altomare, G. Cascarano, C. Giacovazzo, and A. Guagliardi, *J. Appl. Cryst*., 1993, **26**, 343.

48. CrystalStructure 4.1: Crystal Structure Analysis Package; Rigaku Corporation (2000-2014). Tokyo 196-8666, Japan.
49. SHELXL Version 2016/6: G. M. Sheldrick, *Acta Cryst*., 2008, **A64**, 112.